Luo, M., Shi, G. R., Hu, S., Benton, M. J., Chen, Z. Q., Huang, J., Zhang, Q., Zhou, C., & Wen, W. (2017). Early Middle Triassic trace fossils from the Luoping Biota, southwestern China: Evidence of recovery from mass extinction. *Palaeogeography, Palaeoclimatology, Palaeoecology*. https://doi.org/10.1016/j.palaeo.2017.11.028

Early Middle Triassic trace fossils from the Luoping Biota, southwest China: evidence of recovery from mass extinction

Mao Luo[a, b, c, *], G. R. Shi[a], Shixue Hu[d], Michael J. Benton[e], Zhong-Qiang Chen[b,**], Jinyuan Huang[d], Qiyue Zhang[d], Changyong Zhou[d], Wen Wen[d]

[a]*Deakin University, Geelong, Australia. School of Life and Environmental Sciences & Centre for Integrative Ecology, (Burwood Campus). 221 Burwood Highway, Burwood Victoria, 3125*

[b]*State Key Laboratory of Biogeology and Environmental Geology, China University of Geosciences, Wuhan 430074, China*

[c]*State Key Laboratory of Geological Processes and Mineral Resources, China University of Geosciences, Wuhan 430074, China*

[d]*Chengdu Centre of China Geological Survey, Chengdu 610081, China*

[e]*School of Earth Sciences, University of Bristol, Bristol, BS8 1RJ, UK*

**Email address: m.luo@deakin.edu.au (M. Luo), zhong.qiang.chen@cug.edu.cn (Z.Q. Chen)

Abstract

Trace fossils have proven useful for studying the timing and process of biotic recovery after the Permian–Triassic Mass Extinction (PTME). Recovery stages are defined by comparing successive ichnoassemblages from the latest Permian to the early Middle Triassic. Lower Triassic trace fossils have been explored in some detail, but those of the lower Middle Triassic are less well known. Here, well-preserved fossil materials from the Luoping Biota from Yunnan Province, South China suggest that a fully recovered shallow marine ecosystem was re-established by the early Middle Triassic. Trace fossil assemblages of the Luoping Biota are characterized by high ichnodiversity, with 14 ichnogenera in the shallow marine environment of an intra-carbonate platform basin, and nine ichnogenera in the subtidal environment. Such moderate to high ichnodiversity, together with a marked increase in burrow sizes and the common occurrence of key ichnotaxa (e.g. *Rhizocorallium* and *Thalassinoides*) suggest that the ichnofauna had reached recovery stage four. In contrast, non turbiditic strata of the offshore setting record only three ichnogenera, with bioturbation indices never exceeding one. Periodic anoxia in bottom waters was presumably the main control for such a protracted trace fossil recovery in an offshore setting, which otherwise aided the fine preservation of body fossils of the Luoping Biota. Furthermore, event sedimentation (turbidite deposits) in the offshore setting incorporates moderate ichnodiversity and moderate to high bioturbation indices, both interpreted as a result of short-term colonization by transported infaunal animals from proximal settings. The occurrence of variable crustacean traces (e.g. *Sinusichnus*, *Spongeliomorpha*, and *Thalassinoides*) at Luoping and the locomotion traces of marine reptiles, together with abundant fishes and fossil decapods, highlights the value of trace fossils in ecosystem reconstruction after the PTME.

Keywords: biotic recovery, ichnological parameter, Guanling Formation, Yunnan, South China

1. Introduction

The Permian–Triassic Mass Extinction (PTME), with approximately 90% loss of marine invertebrate and ~ 80% of terrestrial vertebrate species, is considered the most severe in its ecological impact on both marine and continental ecosystems (Erwin et al., 2002; Erwin, 2006; McGhee et al., 2004). It was not until the early Middle Triassic that fully recovered shallow marine ecosystems were re-established (Chen and Benton, 2012). The PTME and subsequent recovery have been widely studied, with key questions regarding the extinction mechanism and recovery process remaining open for continued research (Chen and Benton, 2012; Foster and Twitchett, 2014).

Trace fossils have proven useful as a means of deciphering the timing and patterns of biotic recovery after the PTME (Twitchett and Wignall, 1996; Pruss and Bottjer, 2004; Twitchett, 2006; Chen et al., 2011, 2012; Hull and Darroch, 2013). Trace fossils provide invaluable information regarding biotic perturbations that is not readily available through geochemical, sedimentological, and modelling-based studies (Morrow and Hasiotis, 2007; Zonneveld, 2011). Trace fossils represent the activities of both skeletonized and soft-bodied organisms. Soft-bodied organisms account for a large percentage of the total biomass within marine ecosystems (Allison and Briggs, 1991; Sperling, 2013), but are typically only preserved in the form of trace fossils. Hence, ichnofossils potentially provide more complete records of the behaviours of both infaunal and epifaunal organisms than do body fossils, thus facilitating the study of community structures and composition (Morrow and Hasiotis, 2007).

Lower Triassic trace fossils from all over the world have been studied extensively, yielding key data on the timing and process of recovery of trace-making organisms from the PTME (e.g. Twitchett and Wignall, 1996; Twitchett, 1999; Pruss and Bottjer, 2004; Twitchett and Barras, 2004; Beatty et al., 2008; Fraiser and Bottjer, 2009; Chen et al., 2011; 2012, 2015; Zonneveld et al., 2010; Knaust, 2010; Hofmann et al., 2011; 2015; Luo, 2014; Luo and Chen, 2014; Shi et al., 2015; Baucon and Carvalho, 2016; Luo et al., 2016; Feng et al., 2017a, b). Recovery stages were defined by comparing ichnological parameters of locally studied ichnoassemblages from the Early Triassic with those from the latest Permian and early Middle Triassic (e.g. Twitchett and Barras, 2004; Twitchett, 2006; Zonneveld et al., 2010; Pietsch and Bottjer, 2014). These comparisons suggest a step-wise recovery of trace-making organisms, as documented by the gradual increase in ichnodiversity, burrow size, tiering level, and the appearance of key ichnotaxa, from the Griesbachian to Spathian (Twitchett, 2006; Pietsch and Bottjer, 2014). Meanwhile, highly diverse ichnoassemblages discovered in the earliest Triassic suggest the presence of refugia in certain high-latitude regions and some potential equatorial regions, which facilitated a faster recovery of trace makers (e.g. Zonneveld et al., 2010; Knaust, 2010; Godbold et al., 2017).

Despite these intensive ichnological studies of Lower Triassic successions around the world, relatively little attention has been paid to trace fossils from the pre- and post-recovery intervals (Wignall et al., 1995, 1998; Zonneveld et al., 2001; Zhao et al., 2010; Ding et al., 2016; Uchman et al., 2016; Feng et al., 2017c), in order to better understand the timing and pattern of biotic recovery.

Recently, the lower Middle Triassic Guanling Formation from Luoping County in Yunnan province, Southwestern China has attracted substantial attention for the discovery of the Luoping Biota (Zhang et al., 2008a; 2009; Hu et al., 2011; Chen and Benton, 2012; Feldmann et al., 2012, 2015; Wen et al., 2012, 2013; Benton et al., 2013; Huang et al., 2013; Liu et al., 2014; Schweitzer et al., 2014; Zhang et al., 2014). Prolific vertebrate and invertebrate fossils from this biota record a well-developed shallow marine ecosystem in the middle–late Anisian, suggested as marking the final stage of recovery after the PTME (Hu et al., 2011; Chen and Benton, 2012; Benton et al., 2013; Liu et al., 2014). Meanwhile, trace fossils (including coprolites) are similarly well preserved in association with body fossils in the Luoping Biota. They provide an extraordinary window into the behaviours of trace-making organisms from a stabilized, fully recovered shallow marine ecosystem after the PTME. Although some exceptionally preserved examples of coprolites and paddle imprints of nothosaurs from the Luoping Biota sites have been recently studied (Hu et al., 2011; Zhang et al., 2014; Luo et al., 2017), most of the burrowing traces remain unstudied.

Accordingly, this paper aims to document this trace fossil assemblage from the Luoping Biota, and compare it with those from Lower Triassic successions of South China and other regions of the world. The possibility of using the Luoping trace fossil records as a template to interpret the timing of recovery of trace-making organisms is also explored.

2. Geological setting, stratigraphy and depositional environment

2.1. Geological setting and stratigraphy

The three studied sections are located in Luoping County, eastern Yunnan Province, Southwest China (Fig. 1). During the early Middle Triassic, Luoping, together with its border areas between eastern Yunnan and western Guizhou Provinces, was located on the southwestern part of the Yangtze Platform and separated from the Nanpanjiang Basin by a shoal complex (Feng et al., 1997; Lehrmann et al., 2005; Enos et al., 2006; Fig. 1B). Within the vast Yangtze Platform interior, several spatially and temporally separated intraplatform basins or depressions with exceptional fossil preservation, namely the Panxian, Luoping, Xingyi, and Guanling, have been recognized from the late Anisian, late Ladinian and Carnian intervals, respectively (Hu et al., 2011; Benton et al., 2013). These basins shared similar features, including restricted circulation, density stratification of the water column, and dysoxic to anoxic bottom waters during the burial of these exceptionally preserved vertebrate faunas through various stages of the Triassic (Benton et al., 2013). At Luoping, abundant marine reptile faunas were preserved in a basinal setting represented by the upper part of Member II of the Guanling Formation (Hu et al., 2011). The highly fossiliferous, dark micritic limestone of the upper part of Member II can be traced over an area of around 200 km^2 (Benton et al., 2013). Member I and the lower–middle parts of Member II of the Guanling

Formation record similar successions over the entire Yangtze Platform interior region in the Yunnan-Guizhou border areas (Enos et al., 2006; Feng et al., 2017b, 2017c).

The Guanling Formation is subdivided into two members. Member I is dominated by siliciclastic sediments representing deposition in subtidal to intertidal environments (Hu et al., 1996), whereas Member II comprises micritic limestone, bioclastic limestone, oncoidal limestone and dolomite in the lower and middle parts, and black muddy limestone, cherty limestone, and grey dolomite in the upper part. Integration of sedimentary facies analysis, palaeontology and taphonomy indicates that the lower and middle parts of Member II were deposited in relatively open, shallow marine settings, whereas the upper portion of the member was deposited in a low-energy, semi-enclosed intraplatform basin influenced by episodic storms (Hu et al., 2011). The Guanling Formation in the Luoping area, overall, records a progressively deepening succession (Zhang et al., 2008a).

The *Nicoraella kockeli* Conodont Zone has been detected in the upper part of Member II. This conodont zone includes elements, such as *Nicoraella germanicus*, *Nicoraella kockeli* and *Cratognathodus* sp., indicative of the Pelsonian age of the middle Anisian (Zhang et al., 2009). The underlying Member I of the Guanling Formation yields the bivalves *Myophoria* (*Costatoria*) *goldfussi mansuyi* Hsü, *Unionites spicatus* Chen, *Posidonia* cf. *pannonica* Moj, and *Natiria costata* (Münster), and contains several clay beds. This bivalve assemblage is of early Anisian age in South China (Zhang et al., 2008a), and the clay beds have been regarded as correlation markers for the base of the Anisian in southwest China (Enos et al., 2006; Zhang et al., 2009).

2.2. Interpretation of depositional environment

Three sections have been excavated systematically at Luoping for fossil collection and study of the stratigraphy and depositional environment. They are named Dawazi (or Daaozi) (DWZ), Shangshikan (SSK), and Xiangdongpo (XDP), respectively (Zhang et al., 2008a; 2009; Huang et al., 2009; Bai et al., 2011; Hu et al., 2011; Figs. 1A, 2). The Middle Triassic successions in these three excavation sites correlate well with each other by a sharply based, bioturbated wackestone separating the upper and lower fossiliferous units (Bai et al., 2011; Zhang et al., 2014). Further, the three sections are located close together, and individual limestone marker beds can be traced across country between the sections. The thickly bedded limestone unit bears extremely consistent features, including thorough bioturbation, the inclusion of burrows filled by silica concretions, and almost uniform thickness, thus serving as a clear marker unit. Following this recognition, three stratigraphic units have been defined and correlated in the three sections. The documented sedimentary features of these units and their environmental interpretations are as below.

2.2.1. Unit A (shallow to deep subtidal)

Unit A is composed of medium-to thick-bedded bioclastic wackestone and oncoidal pack-wackestone with a small proportion of calcareous mudstone (Fig. 3A, G, H). In DWZ and SSK, stromatolitic bindstones also occur as major constituents. Fragmented bivalve shells, echinoderms, and ostracods are the main skeletal components in wackestone and packstone, with faecal pellets as subordinate grain types. Planar lamination is well developed in both wackestone and carbonate mudstone facies, with bioturbation index (BI) ranging from 1 to 4 (BI schemes follow Reineck, 1963, and Taylor and Goldring, 1993). BI 1 represents sparse disruption of sediments (1–4%) whereas BI 4 is characterized by intense bioturbation (61–90%). Wavy crinkled lamination developed locally in the dolomitic limestone (Fig. 3H)

The dominance of muddy facies in this association indicates a deep subtidal setting. Oncoids indicate moderate energy conditions in shallow water. Stromatolitic build-ups have been observed from shallow to deep subtidal environments in the Triassic (e.g. Flügel et al., 2004, p. 57; Ezaki et al., 2008, 2012). Thus, a shallow to deep subtidal setting is interpreted for Unit A.

2.2.2. Unit B (offshore)

Unit B is composed mainly of very thin bedded (1–3 cm) marly carbonate mudstones intercalated with very thin-bedded (1 cm) black shales (Fig. 3B–C), bioturbated wackestones, and minor thin-bedded packstones. Thin bedded to lenticular chert layers and cherty nodules are also prominent. Planar lamination and reticulated ridge structures (Fig. 3B–C; Luo et al., 2013) are pervasively developed in marly carbonate mudstones, followed by locally occurring convolute lamination. Disseminated pyrite crystals and pyrite framboids are common in marly carbonate mudstones (Fig. 8A, C), in which bioturbation is absent except for a few surficial trails preserved on bedding planes. Locally, normally graded packstone beds have a basal sharp and erosive contact, which are overlain by planar to convolute lamination and massive carbonate mudstones (Fig. 3D). These coarse-grained beds are also characterized by pervasive bioturbation. Thick-bedded, sharp-based nodular (bioturbated) wackestone marker layers separate the upper and lower marly carbonate mudstone beds/units (Fig. 3E), in which abundant well-preserved vertebrate and invertebrate fossils have been discovered, respectively (Fig. 2; Bai et al., 2011; Benton et al., 2013; Zhang et al., 2014; Luo et al., 2017). Several ash layers also occur intercalated in the marly carbonate mudstones of Unit B (Fig. 2).

The overall fine-grained sediments of Unit B are interpreted as deposits from suspension in a low-energy environment with weak current activity. This is shown by the thinly laminated nature of the marly carbonate mudstones and shales. Reticulated ridge structures have been interpreted as indications of benthic microbial mats (Luo et al., 2013). The wide occurrence of benthic microbial mats required a water depth within the photic zone, the lower limit of which is 80–100 m (e.g. James and Bourque, 1992, p. 326). The packstone beds, with their overlain planar/convolute-laminated sediments and massive carbonate mudstones represent Ta, Tb and Te of the Bouma Sequence, which are interpreted to be the result of low-density, dilute turbiditic currents (e.g. Walker, 1992). Similar thin-bedded turbidite deposits have also been observed in the Meride Limestone of the Monte San Giorgio Lagerstätte (Stockar, 2010). Furthermore, turbidite current activity is further supported by the bedded nature of the chert beds, which is interpreted as the result of rapid, turbiditic input of biogenic sediments (e.g. McBride and Folk, 1979; Bustillo and Ruiz-Ortiz, 1987). The common occurrence of pyrite framboids in the carbonate mudstones possibly indicates anoxic bottom water conditions. To sum up, Unit B represents deposition in an anoxic offshore environment.

2.2.3. Unit C (offshore transition)

Unit C is composed of thin- to medium-bedded hummocky cross-stratified wackestones (Fig. 3F), carbonate mudstones, with minor intraclastic floatstones and bioclastic packstones. Wackestone beds are sharply to erosively based, with a few cherty nodules present locally. Convolute lamination and gutter casts also occur. Bioturbation is pervasive in the wackestones and carbonate mudstones. Intraclasts are composed of carbonate mudstone. Packstone layers are lenticular and have graded bedding in the basal parts.

Packstones with a graded basal part, together with their lenticular morphology are most likely associated with storms. Such storm activity is also indicated by the frequent occurrence of hummocky cross-stratification, which is interpreted as a combination of waning oscillatory flow and unidirectional currents created by periodic storm events (Dott and Bourgeois, 1982;

Dumas and Arnott, 2006). Thus, Unit C is interpreted as the deposits of an offshore transitional environment.

3. Ichnological features of the Luoping Biota

Fourteen ichnotaxa have been identified from the three studied sections through Member II of the Guanling Formation. These ichnotaxa are distributed in both the lower and upper fossil layers and strata above and below (Fig. 2). Detailed descriptions of all discovered trace fossils and ichnological parameters are presented below.

3.1. Ichnological descriptions

3.1. Archaeonassa *Fenton and Fenton, 1937*

3.1.1. Archaeonassa fossulata *Fenton and Fenton, 1937 (Fig. 4A)*

Preserved as concave epirelief on upper bedding plane of carbonate mudstone. Grooved trails are gently curved, and are flanked by rounded ridges. Width of trail is about 10 mm and length up to 230 mm. Width remains consistent in individual trails.

Remarks: The grooved trail flanked on both sides by rounded ridges is diagnostic of *Archaeonassa* (Fig. 4A). Although the observed specimen from the DWZ section is similar to *Helminthopsis*, the meandering characteristics of *Helminthopsis* are more complicated than those of *Archaeonassa*. *Archaeonassa* is typically preserved in intertidal regimes where such traces may be abundant (Fenton and Fenton, 1937), and it may also occur more rarely in shallow marine environments. *Archaeonassa* is also known from continental environments (e.g. Buckman, 1994; Buatois and Mángano, 2002). *Archaeonassa* can be produced by various invertebrates, including molluscs and arthropods (Buckman, 1994; Yochelson and Fedonkin, 1997).

3.2. Arenicolites *Salter, 1857*

3.2.1. Arenicolites isp. *(Fig. 4B)*

Preserved as paired tubes on upper bedding planes of carbonate mudstones and wackestones. Tubes are preserved as hollow, funnel-shaped openings with no burrow fill or probably eroded away. Tube diameters range from 7 to 18 mm and the distance between the tubes (width) is up to 62 mm. Diameters of the two tubes in a pair are slightly different.

Remarks: *Arenicolites* and *Skolithos* are difficult to distinguish when they occur densely on bedding planes. The tube structures are usually paired, justifying a reasonable assignment to *Arenicolites*. No spreiten structures have ever been observed between the paired tubes, excluding their assignment to *Diplocraterion*. *Arenicolites* is regarded as an element of the shallow marine *Skolithos* ichnofacies and firmground *Glossifungites* ichnofacies (e.g. Buatois and Mángano et al., 2011a; MacEachern et al., 2012), although such biogenic structures also occur in freshwater deposits (Bromley and Asgaard, 1979). Trace producers include various worm-like organisms, such as polychaetes (Bradshaw, 2010).

3.3. Dikoposichnus *Zhang et al., 2014*

3.3.1. Dikoposichnus luopingensis *Zhang et al., 2014 (Fig. 4C)*

Large, narrow V-shaped slot-like depressions preserved as single or paired imprints on both upper bedding plane (concave epireliefs) and sole surfaces (convex hyporeliefs). Individual imprint is elliptical to sigmoidal, with an anterior sweep at the medial edge. Paired imprints commonly consist of long (up to 18.7 m) trackways that are 30–70 cm wide.

Remarks: This new trace was introduced by Zhang et al. (2014) based on materials from bed 107 of the DWZ section. The well-preserved footprints in long trackways are paired, suggesting the limbs moved in concert. They were interpreted as the paddle imprints of a limbed vertebrate (e.g. nothosaur) moving in a steady manner over the seabed searching for prey (Zhang et al., 2014). It is considered to represent the first locomotion record of marine reptiles from the Mesozoic.

3.4. Diplocraterion *Torell, 1870*

3.4.1. Diplocraterion isp. *(Fig. 4D–F)*

Paired tubes with variable size ranges in both burrow width and diameter. Maximum burrow diameter can reach 17.5 mm and width of up to 84 mm. There are very delicately preserved spreiten structures within shafts connecting the two tubes. Burrow fill of tubes and connected shafts have a darker colour than the host rock.

Remarks: In plan view, the dumbbell-shaped structure, in which the paired tubes are linked by spreiten, justifies assignment to *Diplocraterion*. There is no further evidence of detailed structures in vertical profiles, which prevents assignment to an ichnospecies. Features of the spreiten that connect the paired tubes suggest it is protrusive, indicating a downward movement of trace makers in response to possible erosion of the sediment surface (Bromley, 1996; Buatois and Mángano, 2011a). Dense preservation of these burrows as patch assemblages indicates some possible opportunistic strategies of the trace makers (e.g. Vossler and Pemberton, 1988). In particular, variably sized *Diplocraterion* occurring together could be the product of different generations of animals. *Diplocraterion* is regarded as a dwelling trace of suspension feeders and has a stratigraphic range from Cambrian to present (Abbassi, 2007). It is a characteristic member of the *Skolithos* ichnofacies, and also the substrate-controlled *Glossifungites* ichnofacies (MacEachern et al., 2007; Buatois and Mángano, 2011a). It has also been utilized for defining sequence boundaries and stratigraphic correlation (Taylor and Gawthorpe, 1993; Olóriz and Rodríguez-Tovar, 2000).

3.5. Megagrapton *Książkiewicz, 1968*

3.5.1. Megagrapton irregulare *Książkiewicz, 1968 (Fig. 4G)*

Cord-sized strings preserved as convex hyporeliefs; burrows meander irregularly and branching at right angles. Meandering burrows also form irregular, rectangular meshes that are not closed.

Remarks: The specimen observed at Luoping has diagnostic features including perpendicular branching angles and unclosed meshes resembling *Megagrapton irregulare*. *Megagrapton* is a typical ichnotaxon of flysch strata, usually preserved on sole surfaces in association with other graphoglyptids. It bears some characteristics resembling *Protopaleodictyon* (Książkiewicz, 1977; Uchman, 1998). *Megagrapton* has been commonly observed in Permian to Cretaceous flysch strata in China (e.g. Zhang et al., 2008b).

3.6. Palaeophycus *Hall, 1847*

3.6.1. Palaeophycus isp. *(Fig. 5A)*

Simple, horizontal to inclined cylindrical burrows preserved in carbonate mudstones. Burrows are straight to slightly curved, sub-circular in cross-section. The burrow wall is smooth, and burrow width ranges from 8 to 13 mm. Burrow linings are typical. Burrow fill is the same in colour and composition as the host rock.

Remarks: The similarity of the burrow fill and the surrounding host rock and burrow lining are typical of the ichnogenus *Palaeophycus* (e.g. Osgood, 1970; Pemberton and Frey, 1982). *Palaeophycus* is a facies-crossing ichnogenus and occurs from the Precambrian to present (Pemberton and Frey, 1982).

3.7. Planolites *Nicholson, 1873*

3.7.1. Planolites isp. (Fig. 5B)

Horizontal, smooth trails that are straight to gently curved. They are circular to elliptical in transverse section. Burrows are unbranched, and commonly cross-cut each other. Burrow fill is structureless, and is darker than the host rock. Burrow diameters range from 2.1 to 25.1 mm, and average 10.5 mm.

Remarks: The unlined burrow and its darker colour in contrast to the host rock is diagnostic of *Planolites*. It is a facies-crossing ichnotaxon, ranging through a wide variety of environments from shallow to deep marine and also nonmarine. Its producer includes certain vermiform deposit feeders (e.g. Pemberton and Frey, 1982; Uchman, 1995). *Planolites* also has a wide stratigraphic range from the Precambrian to present (Häntzschel, 1975).

3.8. Rhizocorallium *Zenker, 1836*

3.8.1. Rhizocorallium isp. *(Fig. 5C)*

Gently inclined to horizontal, U-shaped tubes are preserved as full reliefs in carbonate mudstones/wackestones. U-tube has dark burrow fill in contrast to the host rock (Fig. 5C). No spreiten structures are evident between limbed tubes. Burrow size (width of U tube) ranges from 16 to 43 mm, with an average value of 26.1 mm (Fig. 7C). Clustered individuals cross cut-each. They are also found to cross-cut the previously formed, meshwork burrowing systems resembling *Thalassinoides*.

Remarks: Specimens from the Guanling Formation in the Luoping area bear certain characteristics resembling *Rhizocorallium commune* (Knaust, 2013). These include their gregarious nature, the relatively smaller size compared with *R. jenense* (see below), and their cross-cutting relationships. However, the absence of scratches along marginal tubes prevents unequivocal assignment. *Rhizocorallium* can be produced by various animals including decapods, crustaceans, annelids, polychaetes, and also mayflies (Knaust, 2013).

3.8.2. Rhizocorallium jenense *Zenker, 1836 (Fig. 5D–F)*

These U-shaped burrows are isolated, and preserved as horizontal epirelief or hyporeliefs. Burrow fill has similar colour to the host rock. Typical spreiten structures between the limbed tubes are characteristic (Fig. 5D–E). The whole U-shaped tubes form long tongue-shaped structures and even complex spiral burrowing systems. Ornamented faecal pellets are evident in limbed burrows (Fig. 5F). Burrow width of U-tubes ranges from 27 to 74.5 mm, and averages 51.3 mm (Fig. 7B).

Remarks: These specimens are assignable to *Rhizocorallium jenense*, which is characterized by an elongate morphology, larger size and prominent faecal pellets in limbed tubes. *Rhizocorallium* is an element of the *Cruziana* ichnofacies and also a representative ichnotaxon of the firmground *Glossifungites* ichnofacies (Buatois and Mángano, 2011a). *Rhizocorallium* has been widely recognized in strata from the lower Cambrian to Cenozoic (e.g. Knaust, 2013). The potential producer of *R. jenense* could be a polychaete (Knaust, 2013).

3.9. Sinusichnus *Gibert, 1996*

3.9.1. Sinusichnus isp. *(Fig. 5G–H)*

This trace is preserved as positive or negative hyporeliefs, and can be found over areas spanning several square decimetres. Horizontal burrows are knobbly, and show regular sinuous tunnels, but less regular to straight tunnels are also evident/present in the same branching system (Fig.5G). Branching points usually comprise three points forming a Y- or T-shaped junction (Fig. 5G). In some cases, two closely emplaced triple junctions form an H-like configuration. Four-pointed branching is also apparent locally. The burrow system penetrates into the sediment at very shallow depths (no more than 1.5 cm). Retrusive spreiten were not observed. Diameters of sinuous burrows remain identical in each distinct burrow system, but vary slightly between different specimens. Measurements of 102 specimens reveal a burrow width ranging from 4 to 16 mm, with an average value of 8.8 mm.

Remarks: The newly discovered traces are extremely similar to the ichnogenus *Sinusichnus* established by Gibert (1996). This is revealed by the regular sinuous and branching morphology of the horizontal tunnels. In addition, the significant relationship between wavelength (λ) and amplitude (A) in the Luoping specimens has also been found in typical *S.sinuosus* (Gibert et al., 1999a). Apart from the type ichnospecies *S. sinuosus* established by Gibert (1996), Kapper (2003) proposed another ichnospecies, *S. priesti*, based on specimens from Upper Cretaceous strata in Germany. The only feature distinguishing *S. sinuosus* from *S. priesti* is the presence of bioglyphs in the latter. No scratch marks or bioglyphs are evident on the branching burrows observed herein. In addition, the knobbly appearance of the specimen suggests some lining of the burrows, a feature that is not present in *Sinusichnus*. It is noted also that the specimens studied here are less regular in some parts of the burrow segments compared with those from Pliocene and Miocene strata (e.g. Buatois et al., 2009; Belaüstegui et al., 2014). These features make it difficult to assign the specimen to any of the ichnospecies established. The trace *Sinusichnus* can be produced by decapod crustaceans and isopods, and has a stratigraphical range from Middle Triassic to Pliocene (e.g. Gibert, 1996; Buatois et al., 2009; Belaüstegui et al., 2014; Knaust et al., 2016).

3.10. Spongeliomorpha *Saporta 1887*

3.10.1. Spongeliomorpha isp. *(Fig. 6A)*

This trace is preserved as full relief on the upper surface of carbonate mudstones. Burrows exhibit Y-shaped branching, with delicate, longitudinal scratch marks seen on burrow wall surface. There is enlargement at burrow intersection. Burrow diameter ranges from 21 to 27 mm.

Remarks: The observed specimens bear characteristics, such as Y-shaped branching and scratched burrow walls, typical of *Spongeliomorpha*. However, it should be noted that the longitudinal striae (scratch marks) are different from the transversely oriented striations reported in some previous work (e.g. Bromley and Asgaard, 1979), nor are they comparable with those observed in *S. iberica* (e.g. Melchor et al., 2009). An assignment at ichnospecies level is unresolved. Although several animals have been proposed as the possible trace makers of *Spongeliomorpha*, the enlargement at the bifurcating junction, together with scratch marks on the burrow wall surface, indicate that a decapod is most likely the trace maker for *Spongeliomorpha* isp. at Luoping. This trace has been found in both marine and nonmarine environments, and has a stratigraphical range from Early Permian to Miocene (Bromley and Asgaard, 1979; Carmona et al., 2004; Melchor et al., 2009).

3.11. Taenidium *Heer 1877*

3.11.1. Taenidium barretti *Bradshaw, 1981 (Fig. 6B)*

Unlined cylindrical burrow preserved in carbonate wackestone. In vertical profile, sinuous burrows contain dark, articulated burrow fill alternating with light meniscate partings. The alternating two types of sediment have varying thickness and are unevenly spaced. Burrow is unbranched, and has a consistent diameter of 10 mm.

Remarks: The specimen has a striking resemblance to *Beaconites antarcticus* as illustrated by Graham and Pollard (1982). However, following the reclassification of *Beaconites*, *Taenidium* and *Ancorichnu*s (Keighley and Pickerill, 1994), this trace fossil should be renamed as *Taenidium barretti*. The taxonomy of meniscate burrows was comprehensively reviewed and revised by D'Alessandro and Bromley (1987). Three ichnospecies were proposed as valid for *Taenidium* before *Taenidium barretti*, namely *T. serpentinum, T. cameronensis, and T. satanassi* (D'Alessandro and Bromley, 1987). The unbranched, meniscate structures observed herein have very gentle curvature, and consist of unevenly distributed dark and light menisci that are deeply arcuate and tightly packed. These features justify assignment to *Taenidium barretti*. *Taenidium* has been reported from strata ranging from the Cambrian to Eocene (D'Alessandro et al., 1986; D'Alessandro and Bromley, 1987; Yang et al., 2004), but most occurrences are from the Silurian–Devonian, and the Cretaceous to Eocene (e.g. Häntzschel, 1975, p.W84; Bradshaw, 1981).

3.12. Thalassinoides *Ehrenberg, 1944*

3.12.1. Thalassinoides suevicus *Rieth, 1932 (Fig. 6C)*

The burrows are preserved as either concave epirelief or convex hyporelief on carbonate mudstones/wackestones. Burrows typically occur as Y-shaped branching systems and have swollen bumps at conjunction points (Fig. 6C). Burrow surface is smooth. Burrow sizes range from 5 to 30 mm, and average 17.9 mm. Burrow shafts usually form complicated meshworks covering a maximum area of up to tens of square metres. Burrow penetration depth is shallow (no more than 5 cm). On some horizons of the XDP section, larger Y-shaped burrows systems were cross-cut by U-shaped *Rhizocorallium* isp.

Remarks: This trace is characterized by its Y-shaped branching. The swollen part at the junctions implies that these *Thalassinoides* traces were produced by decapod crustaceans (Bromley and Frey, 1974; Carmona et al., 2004; Carvalho et al., 2007). Such a trace fossil is usually interpreted as a dwelling or feeding structure produced by detritus-feeding crustaceans in shallow to deep marine environments (Myrow, 1995; Carvalho et al., 2007). Besides, *Thalassinoides* burrows are also present in the firmgound substrate of the *Glossifungites* ichnofacies immediately after the end-Permian crisis (Chen et al., 2015). *Thalassinoides* has a stratigraphical range from Cambrian to present (Myrow, 1995), but a decapod origin of such traces has been suggested for Devonian examples (e.g. Carmona et al., 2004).

3.13. Undichna *Anderson, 1976*

3.13.1. Undichna unisulca *Gibert et al., 1999 (Fig. 6D)*

These are unpaired sinuous ridges on sole surfaces of bedding planes of wackestones/packstones. Two single trails were identified, which are preserved as regular sinusoidal strings with equal wavelength and amplitude. The sinuous trail is composed of two to three ridges separated by subtle grooves.

Remarks: The Luoping specimens of single-waved trails are extremely similar to *Undichna unisulca* diagnosed by Gibert et al. (1999b) and Morrissey et al. (2004) in both morphology and preservation, and thus justify assignment to this ichnospecies. This trace has been interpreted to be generated by a fish swimming with its caudal fin in contact with the substrate (Gibert et al, 1999b). As fishes diversified from the Ordovician onwards, their behavioural product, *Undichna* also has a very wide stratigraphic distribution in the

Palaeozoic, Mesozoic and Cenozoic (Gibert et al., 1999b., Gibert, 2001; Benner et al., 2009; Fillmore et al., 2011).

3.14. Zoophycos *Massalongo, 1855*

3.1.14. Zoophycos isp.? *(Fig. 6E, F)*

These are spiral-shaped structures composed of U-shaped protrusive, primary laminae of variable orientation. Primary laminae arrange in helicoid spirals to form an overall elliptical shape, with no marginal tubes observed.

Remarks: The primary laminae forming helicoid spirals is characteristic of *Zoophycos* (e.g. Uchman, 1995), but the incomplete preservation of the specimen and absence of marginal tubes prevent assignment to an ichnospecies. The origin of *Zoophycos* is unresolved, although it is generally assumed to have been made by deposit-feeding organisms (Uchman, 1995; 1998), with sipunculoids, polychaete annelids, and enteropneust hemichordates all possible trace makers (e.g. Wetzel and Werner, 1981; Ekdale and Lewis, 1991; Kotake, 1992). *Zoophycos* has a stratigraphic age range from Cambrian to present (e.g. Zhang et al., 2015), and its trace maker transferred from shallow water environments in the Palaeozoic to deep marine environments since the Cretaceous (e.g. Seilacher, 1974; Zhang et al., 2015).

4. Eco-ichnological characteristics

4.1. Abundance and ichnodiversity

Fourteen ichnogenera were recorded from the three studied sections at Luoping. Among these, six ichnogenera are more abundant than the others, and these form dense assemblages at particular horizons. These are *Arenicolites*, *Dikoposichnus*, *Diplocraterion*, *Planolites*, *Rhizocorallium*, and *Thalassinoides*. Other traces are only locally developed.

The offshore setting of Unit B is characterized by very low ichnodiversity and low BI. Non-turbiditic strata, as represented by marly carbonate mudstone and shales are nearly devoid of bioturbation, with only *Dikoposichnus*, *Megagrapton* and *Undichna* preserved as surficial trails/tracks on bedding planes. It is the same case for both the upper and lower ‘fossil horizons'. The sharply to erosively based turbidite beds, in contrast, have a moderate to high BI and a moderately diverse ichnoassemblage. Ichnotaxa in those event beds include *Diplocraterion, Planolites, Rhizocorallium, Sinusichnus, Taenidium,* and *Thalassinoides*. There is a marked increase in BI for the offshore transition of Unit C. Most of the beds were variously bioturbated, with BI ranging from two to four. However, the ichnodiversity remains low. Unit A saw the highest level of both BI and ichnodiversity. Nine ichnogenera were discovered from this unit, including *Archaeonassa*, *Arenicolites*, *Palaeophycus*, *Planolites*, *Sinusichnus*, *Rhizocorallium, Spongeliomorpha, Thalassinoides*, and ? *Zoophycos*. BI levels also increased, from one to four.

4.2. Burrow size

Burrow sizes of the abundantly preserved traces of the Luoping Biota were analyzed statistically. Burrow forms analyzed include *Diplocraterion*, *Planolites*, *Rhizocorallium* and *Thalassinoides* (Fig. 7A–D).

The average burrow width of *Diplocraterion* is 26.4 mm based on measurements of 135 individuals. *Planolites* has a wide range of burrow diameters (2.1–25.1 mm), average 10.5 mm (Fig. 7A). Two ichnospecies of *Rhizocorallium* were measured separately. For the larger group, burrow width of the U-tubes averages 51.3 mm (Fig. 7B), whereas the average width for the smaller one is 26.1 mm. For the mazework of *Thalassinoides*, the burrow widths range from 5 to 30 mm, with a mean value of 17.9 mm, based on 104 measurements (Fig. 7D).

4.3. Tiering level and complexity

Tiering level is practically evaluated by measuring the penetration depth of trace fossils, to explore ecospace utilization of sediment. Trace fossils are preserved at very shallow depths in marly carbonate mudstones of Unit B, where trails, such as *Megagrapton*, *Undichna* and *Dikoposichnus*, occupied only the upper 1–2 cm of the sediments. Vertical burrows, such as *Diplocraterion* and *Arenicolites*, also penetrate to depths of no more than 3 cm. Trace fossils in Unit C also have very shallow penetration depths. Those complex traces such as *Rhizocorallium*, *Spongeliomorpha* and *Thalassinoides*, occupied only the surficial 2–4 cm of the sediments.

Turbidite deposits in Unit B, on the other hand, have deeper burrows than their surrounding non-turbiditic sediments. Vertically oriented *Taenidium* has a penetration depth of 5 cm. The silicified *Thalassinoides* burrows in marked horizons have an even deeper penetration depth up to 10 cm.

5. Discussion

5.1. Decoupled features between trace fossils and body fossils in the Luoping Biota

There is decoupling between the preservation of trace fossils and body fossils at Luoping. In particular, the lower and upper fossiliferous units preserve abundant vertebrate and invertebrate fossils, but with only a few superficial trace fossils, such as *Dikoposichnus*, *Megagrapton*, and *Undichna*. Such a decoupling effect has long been recognized by ichnologists, who explain this phenomenon by differential preservational conditions between trace fossils and body fossils (e.g. Buatois and Mángano, 2011a). Indeed, at Luoping, such decoupling might have resulted from periodic anoxia in offshore environments, which largely inhibited colonization by trace makers. The upper and lower fossiliferous units are both characterized by thin-bedded marly carbonate mudstones intercalated with shales, representing quiet, offshore depositional environments. The black sediments, and the common occurrence of dispersed pyrite crystals suggests possible periodic anoxia in offshore environments. Statistical analysis of the pyrite framboids in carbonate mudstones supports such a notion. Measurements of pyrite framboids from two strata of the lower fossiliferous bed/unit of the SSK section reveal mean diameters of 6.60 μm and 5.34 μm, with standard deviations of 1.21 and 1.77, respectively (Fig. 8A–D). This result indicates an anoxic marine environment (e.g. Wilkin et al., 1996; Wignall and Newton, 1998).

Due to such periodic anoxia in bottom waters, bioturbation was largely inhibited. When there were transient oxic conditions, fishes, marine reptiles, and a few invertebrates could survive and leave their traces of activity, represented by the occurrence of *Undichna*, *Dikoposichnus*, and *Megagrapton*. It is noted that the presence of *Undichna* and *Dikoposichnus*, together with the abundant preservation of fishes and marine reptile fossils in the Middle Triassic Luoping biota may reflect the déjà vu effect (*sensu* Buatois and Mángano, 2011b).

Interestingly, at Luoping, the preservational conditions of the Luoping Biota seem to have aided the preservation of trace fossils in the lower and upper fossiliferous units. Specifically, the sealing effect of microbial mats played a significant role in the preservation of both (including coprolites). When the Luoping animals died and settled on the sea floor, the episodic anoxic environment inhibited rapid decay of the animals. With a further sealing effect from microbial mats, animal carcasses were rapidly coated by mats and protected from disarticulation by turbulent currents (e.g. Luo et al., 2013). Such establishment of firmground substrates might have further stabilized the burrowed sediment surfaces, and enhanced the preservation of those surficial traces (e.g. Buatois and Mángano, 2013).

5.2. Comparison with Early Triassic trace fossil assemblages

A four-stage recovery model based on multiple ichnological parameters has been proposed to summarize the recovery process of trace makers at various stages of the Early Triassic (e.g. Twitchett, 2006), which was later adopted by several researchers (e.g. Chen et al., 2011; Hofmann et al., 2011; Luo et al., 2016). Low ichnodiversity, ichnofabric indices, shallow tiering level and small burrow sizes characterize the early recovery stages (e.g. one to two). This is the case for most ichnoassemblages from shallow marine environments dating from Griesbachian to Dienerian (e.g. Chen et al., 2011; Zhao and Tong, 2010; Zhao et al., 2015). Ichnological parameters show substantial increases in Smithian to Spathian strata from certain regions of South China, eastern Australia, and Western United States, where the recovery stage increased to three or four (e.g. Chen et al., 2011; 2012; Mata and Bottjer, 2011; Luo et al., 2016; Feng et al., 2017). However, not all trace makers had recovered to such an advanced stage in the Smithian and Spathian, suggesting marked variation in recovery rate, most likely controlled by the heterogeneous development of oxic facies (Luo et al., 2016).

At Luoping, nine ichnogenera were discovered from the subtidal deposits of Unit A. Key ichnogenera, such as *Rhizocorallium* and *Thalassinoides* are also commonly found. These observations, together with a moderate to high bioturbation level suggest recovery stage four. Burrow sizes of several ichnogenera (e.g. *Planolites*, *Rhizocorallium* and *Thalassinoides*) also show a marked increase compared with their Lower Triassic counterparts. For example, *Planolites* from subtidal environments at Luoping records a mean diameter of 10.5 mm, which is equivalent to that from the Upper Permian Bellerophon Formation of Northern Italy, obviously larger than Lower Triassic *Planolites* from various regions (e.g. Twitchett, 1999; Pruss and Bottjer, 2004; Zonneveld et al., 2010; Chen et al., 2011; 2012; Luo et al., 2016; Feng et al., 2017a; Fig. 9A), except the late Spathian *Planolites* from the Yashan section of South China (Chen et al., 2011). *Rhizocorallium*is rare in the Lower Triassic, with only a few studies mentioning their burrow sizes. The Induan *Rhizocorallium* from the Montney

Formation of Canada has larger burrow widths even compared to late Early Triassic examples (e.g. Zonneveld et al., 2010; Fig. 9B). This might relate to the presence of refugia in those areas, which facilitate the survival of trace makers. Burrow widths of *Rhizocorallium* from the Smithian Sinbad Limestone, and the Spathian Virgin Limestone of the United States are generally less than 26 mm, with average values of 6 mm and 14 mm respectively (Pruss and Bottjer, 2004; Fraiser and Bottjer, 2009). An obvious increase in *Rhizocorallium* burrow size in the Spathian is also revealed by their occurrence in the Spathian Nanlinghu Formation of the Susong section, South China, and in the Tvilligodden Formation of western Spitsbergen (Worsley and Mørk, 2001; Luo, 2014; Luo et al., 2016). Middle Triassic *Rhizocorallium* from Luoping and other regions of the world (e.g. northwestern British Columbia) have comparable size ranges to their Spathian counterparts (e.g. Zonneveld et al., 2010; Fig. 9B). Burrow sizes of *Thalassinoides* also show obvious increases. Lower Triassic occurrences of *Thalassinoides* from Griesbachian strata of Northern Italy, Western Canada, Smithian strata at Susong in South China, and Spathian strata at Yashan (China) and the Western United States have burrow diameters less than 25 mm (e.g. Zonneveld et al., 2010; Hofmann et al., 2011; Pruss and Bottjer, 2004; Chen et al., 2011; Luo, 2014). The average values for these localities are less than 12 mm (Fig. 9C). At Luoping, the maximum burrow diameter of *Thalassinoides* reaches 30 mm, with the average diameter increasing to 17.9 mm. These values are similar to, or even greater than their Middle to Late Permian counterparts (Whidden, 1990; Zhao and Tong, 2010; Lima and Netto, 2012), and Middle Triassic *Thalassinoides* from north-eastern British Columbia (e.g. Zonneveld et al., 2010; Fig. 9C). In summary, the moderate to high ichnodiversity (nine ichnogenera) in the subtidal environments at Luoping, together with moderate to high bioturation indices, the appearance of key ichnotaxa and increases in burrow sizes, represent a recovery stage four, which suggests a more or less fully recovered ichnossemblage in the early Middle Triassic, 7 Myr after the PTME.

It is worth noting that the bioturbation levels in the turbidite deposits in offshore settings are much higher than their surrounding non-turbiditic strata. In addition, various traces, such as *Diplocraterion*, *Planolites*, *Rhizocorallium*, *Sinusichnus*, *Taenidium*, and *Thalassinoides* were found in those beds. Certain traces, such as *Taenidium*, have penetrated sediments to a depth of 5 cm. Such moderate ichnoassemblages and moderate to high bioturbation levels in turbidite beds are interpreted to be the result of the short colonization of transported infaunal animals from proximal settings (*cf.* Grimm and Föllmi, 1994). The low ichnodiversity and low bioturbation level in non-turbiditic strata of offshore environments at Luoping are most likely due to shallow marine anoxia, and this prevents further comparisons and discussion of their implications for recovery of trace makers in such distal shallow marine settings.

The offshore transition of Unit C in the Luoping sections is associated with low ichnodiversity and moderate bioturbation indices (BI), which is in contrast to the habitable zone model stating that the lower shoreface to offshore transition zone are ideal for colonization (*cf.* Beatty et al., 2008). The low ichnodiversity and moderate BI in the offshore transition at Luoping could partly relate to the topography of the basin and also its proximity to anoxic offshore settings. Several intraplatform basins were formed during the early Middle to Late Triassic at Luoping and its border areas, where well-preserved faunas were discovered (e.g. Hu et al, 2011; Benton et al., 2013). The restricted circulation and density stratification of the water column in these basins means they are not large in scale, and the shelf region in these basins could be narrow and steep. Such bathymetric topography prevented the development of a habitable zone and long-term colonization (*cf.* Zonneveld et al., 2010). In addition, the proximity of the offshore transition to the anoxic offshore setting at Luoping might also have hampered the bioturbating activities of trace makers in this environmental setting through possible upwelling of deeper anoxic waters.

5.3. Implications for ichnofaunal recovery during the Early Triassic

Investigations at Luoping support the utility of trace fossils to study the timing of biotic recovery and the processes of trace makers. The subtidal ichnoassemblage is characterized by medium to high ichnodiversity, medium to high bioturbation indices, and a marked increase in burrow size of many traces. These parameters, together with the common appearance of key ichnogenera (e.g. *Rhizocorallium* and *Thalassinoides*), suggests a recovery stage 4 (*sensu* Twitchett, 2006; Pietsch and Bottjer, 2014), thus indicating a full recovery of trace makers in subtidal environments. Ichnological records from adjacent regions also support an obvious recovery of trace makers (Feng et al., 2017c). In contrast, ichnological parameters from regional ichnoassemblages of Lower Triassic successions typically suggest a recovery stage of one and two, with a few data suggesting some recovery until the latest Smithian and Spathian (Twitchett, 1999; Chen et al., 2011; Zhao et al., 2015; Luo et al., 2016; Feng et al., 2017a). However, the ichnological parameters from offshore environments at Luoping show no signs of recovery. This is most likely due to the periodic anoxic bottom water conditions, which would have substantially inhibited the colonization of infaunal animals, but otherwise aided the fine preservation of the Luoping Biota.

After the PTME, marine ecosystems and ecological structures were re-shaped, with the Modern Evolutionary Fauna expanding to dominate in marine settings (Sepkoski et al., 1981; Erwin, 2006; Peters, 2008). The fossil composition of the Luoping Biota highlights this major change, with fishes, marine reptiles and decapod crustaceans comprising the majority of the fossil collections (e.g. Hu et al., 2011; Wen et al., 2012, 2013; Feldmann et al., 2012, 2015; Huang et al., 2013; Schweitzer et al., 2014). Luoping has revealed many new genera and species of arthropods, which suggest a radiation event during the early Middle Triassic (e.g. Feldmann et al., 2012, 2015, 2017; Huang et al., 2013; Schweitzer et al., 2014). Such a change in ecosystem structure was mirrored by the common occurrence of burrow systems (e.g. *Sinusichnus, Rhizocorallium, Spongeliomorpha,* and *Thalassinoides*) made by decapod crustaceans at Luoping. This highlights how the trace fossil assemblages of the early Middle Triassic document the major faunal changes occurring at this time in comparison with Lower Triassic ichnological records.

6. Conclusions

Well-preserved vertebrates and invertebrates from the Luoping Biota of Yunnan Province in South China suggest a stable, fully recovered shallow marine ecosystem in the early Middle Triassic (Anisian). Equally, well-preserved trace fossils found in association with the Luoping Biota provide a template to compare the behaviours and ecological strategies of trace-making organisms from such a recovered ecosystem with those in the delayed recovery interval of the Early Triassic. Trace fossil assemblages from the Luoping Biota have high ichnodiversity, with 14 ichnogenera discovered in the shallow marine environment of an intra-carbonate platform basin. Nine ichnogenera occurred in the subtidal environment. Such medium to high ichnodiversity, together with a marked increase in burrow size and the common occurrence of key ichnotaxa (e.g. *Rhizocorallium* and *Thalassinoides*) suggest a recovery stage of four. In contrast, non-turbiditic strata of the offshore setting record only three ichnogenera, with bioturbation indices never exceeding one. Periodic anoxic bottom water conditions are identified as the main control on such a protracted trace fossil record, which otherwise aided the fine preservation of body fossils of the Luoping Biota. Furthermore, event sedimentation (turbidites) in offshore settings host a medium ichnodiversity and medium bioturbation indices, both interpreted to result from short term colonization by transported infaunal animals from proximal settings. The occurrence of variable crustacean-made traces (e.g. *Sinusichnus*, *Spongeliomorpha*, and *Thalassinoides*) at Luoping, together with possible evidence of the decapod radiation from body fossils, highlights the value of using trace fossils to document ecosystem restructuring after the PTME.

Acknowledgments

This study was partly supported by the ACRDP discovery grant to G. R. Shi (DP150100690). This research is also supported by two NSFC grants (41572091 and 41772007 to ZQC), two research grants (GBL21410, GPMR201601 to ML) from the State Key Laboratory of Biogeology and Environmental Geology, and State Key Laboratory of Geological Process and Mineral Resources, China University of Geosciences (Wuhan), and China Geological Survey project (DD20160020, 1212011140051, 12120114030601, and 1212010610211). This paper is a contribution to the IGCP 630 “Permian-Triassic climatic and environmental extremes and biotic response”.

References

Abbassi, N., 2007. Shallow marine trace fossils from Upper Devonian sediments of the Kuh-E Zard, Zefreh area, central Iran. Iranian Journal of Science & Technology, Transaction A, 31, 23–33.

Allison, P.A., Briggs, D.E.G., 1991. Taphonomy of non-mineralized tissues. In: Allison, P.A., Briggs, D.E.G. (Eds.), Taphonomy: Releasing the Data Locked in the Fossil Record. Plenum Press, New York, 25–69.

Anderson, A., 1976. Fish trails from the Early Permian of South Africa. Palaeontology 19, 397–409.

Bai, J.K., Yin, F.G., Zhang, Q.Y., 2011. Microfacies and enrichment pattern of fossils in the fossiliferous beds of Luoping Biota, Yunnan Province. Geology in China, 38, 393–402 (in Chinese with English abstract).

Baucon, A., Carvalho, C.N.D., 2016. Stars of the aftermath: *Asteriacites* beds from the Lower Triassic of the Carnic Alps (Werfen Formation, Sauris Di Sopra), Italy. Palaios 31, 161–176.

Beatty, T.W., Zonneveld, J.P., Henderson, C.M., 2008. Anomalously diverse Early Triassic ichnofossil assemblages in northwest Pangea: a case for shallow-marine habitable zone. Geology 36, 771–774.

Belaústegui, Z., de Gibert, J.M., Lopez-Blanco, M., Bajo, I., 2014. Recurrent constructional pattern of the crustacean burrow *Sinusichnus sinuosus* from the Paleogene and Neogene of Spain. Acta Palaenotol. Pol. 59, 461–474.

Benner, J.S., Ridge, J.C., Knecht, R.J., 2009. Timing of post-glacial reinhabitation and ecological development of two New England, USA, drainages based on trace fossil evidence. Palaeogeogr. Palaeoclimatol. Palaeoecol. 272, 212–231.

Benton, M.J., Zhang, Q.Y., Hu, S.X., Chen, Z.Q., Wen, W., Liu, J., Huang, J.Y., Zhou, C.Y., Xie, T., Tong, J.N., Choo, B., 2013. Exceptional vertebrate biotas from the Triassic of China, and the expansion of marine ecosystems after the Permo-Triassic mass extinction. Earth-Sci. Rev. 125, 199–243.

Bradshaw, M.A., 1981. Palaeoenvironmental interpretations and systematics of Devonian trace fossils from the Taylor Group (Lower Beacon Supergroup), Antarctica. New Zealand J. Geol. Geophysics, 24, 615–652.

Bradshaw, M.A., 2010. Devonian trace fossils of the Horlick Formation, Ohio Range, Antarctica: systematic description and palaeoenvironmental interpretation. Ichnos 17, 58–114.

Bromley, R.G., 1996. Trace Fossils. Biology, Taphonomy and Applications. London: Chapman & Hall. 361 pp.

Bromley, R.G., Asgaard, U., 1979. Triassic freshwater ichnocoenoses from Carlsberg Fjord, East Greenland. Palaeogeogr. Palaeoclimatol. Palaeoecol. 28, 39–80.

Bromley, R.G., Frey, R.W., 1974. Redescription of the trace fossil *Gyrolithes* and taxonomic evaluation of *Thalassinoides, Ophiomorpha* and *Spongeliomorpha*. Bull. Geol. Soc. Denmark 23, 311–335.

Buatois, L.A., Mángano, M.G., 2002. Trace fossils from Carboniferous floodplain deposits in western Argentina: implications for ichnofacies models of continental environments. Palaeogeogr. Palaeoclimatol. Palaeoecol 183, 71–86.

Buatois, L.A., Mángano, M.G., 2011a. Ichnology: Organism-Substrate Interaction in Space and Time. Cambridge University Press, New York, 358 pp.

Buatois, L.A., Mángano, M.G., 2011b. The déjà vu effect: recurrent patterns in exploitation of ecospace, establishment of the mixed layer, and distribution of matgrounds. Geology 39, 1163–1166.

Buatois, L.A., Mángano, M.G., 2013. Ichnodiversity and ichnodisparity: significance and caveats. Lethaia 46, 281–292.

Buatois, L.A., Macsotay, O., Quiroz, L.I., 2009. *Sinusichnus*, a trace fossil from Antartica and Venezuela: expanding the datasets of crustacean burrows. Lethaia 42, 511–518.

Buckman, J.O., 1994. *Archaeonassa* Fenton and Fenton 1937 reviewed. Ichnos 3, 185–192.

Bustillo, M.A., Ruiz-Ortiz, P.A., 1987. Chert occurrence in carbonate turbidites: example from the Upper Jurassic of the Betic Mountains (southern Spain). Sedimentology 34, 611–621.

Carmona, N.B., Buatois, L.A., Mángano, M.G., 2004. The trace fossil record of burrowing decapod crustaceans: evaluating evolutionary radiations and behavioural convergence. Fossil and Strata 51, 141–153.

Carvalho, C.N.D., Viegas, P.A., Cachão, M., 2007. *Thalassinoides* and its producer: populations of *Mecochirus* buried within their burrow system, Boca Do Chapim Formation (Lower Cretaceous), Portugal. Palaios 22, 104–109.

Chen, Z.Q., Benton, M.J., 2012. The timing and pattern of biotic recovery following the end-Permian mass extinction. Nat. Geosci. 5, 375–383.

Chen, Z.Q., Fraiser, M.L., Bolton, C., 2012. Early Triassic trace fossils from Gondwana Interior Sea: Implication for ecosystem recovery following the end-Permian mass extinction in south high-latitude region. Gondwana Res. 22, 238–255.

Chen, Z.Q., Tong, J.N., Fraiser, M.L., 2011. Trace fossil evidence for restoration of marine ecosystems following the end-Permian mass extinction in the Lower Yangtze region, South China. Palaeogeogr. Palaeoclimatol. Palaeoecol. 299, 449–474.

Chen, Z.Q., Yang, H., Luo, M., Benton, M.J., Kaiho, K., Zhao, L.S., Huang, Y.G., Zhang, K.X., Fang, Y.H., Jiang, H.S., Qiu, H., Li, Y., Tu, C.Y., Shi, L., Zhang, L., Feng, X.Q., Chen, L., 2015. Complete biotic and sedimentary records of the Permian-Triassic transition from Meishan section, South China: ecologically assessing mass extinction and its aftermath. Earth Sci. Rev. 149, 67–107.

D'Alessandro, A., Bromley, R.G., 1987. Meniscate trace fossils and the *Muensteria-Taenidium* problem. Palaeontology 30, 743–763.

Ding, Y., Cao, C.Q., Zheng, Q.F., 2016. Lopingian (Upper Permian) trace fossils from the northern Penglaitan Section, Laibin, Guangxi, South China and their environmental implications. Palaeoworld 25, 377–387.

Dott, R.H., Bourgeois, J., 1982. Hummocky stratification: significance of its variable bedding sequences. Geol. Soc. Am. Bull. 93, 663–680.

Dumas, S., Arnott, R.W.C. 2006. Origin of hummocky and swaley cross-stratification–the control influence of unidirectional current strength and aggradation rate. Geology 34, 1073–1075.

Enos, P., Lehrmann, D.J., Wei, J.Y., Yu, Y.Y., Xiao, J.F., Chaikin, D.H., Minzoni, M., Berry, A.K., Montgomery, P., 2006. Triassic Evolution of the Yangtze Platform in Guizhou Province, People's Republic of China. Geol. Soc. Am. Special Papers 417, 1–105.

Erwin, D.H., Bowring, S.A., Jin, Y.G., 2002. End-Permian mass extinction: a review. In: Koeberl, C., MacLeod, K.G. (Eds.), Catastrophic events and Mass Extinctions: Impacts and Beyond. Geol. Soc. Am. Special Paper 256, pp. 353–383.

Erwin, D.H., 2006. Extinction: How Life on Earth Nearly Ended 250 Million Years Ago. Princeton University Press, Princeton, 296 pp.

Ezaki, Y., Liu, J.B., Nagano, T., Adachi, N., 2008. Geobiological aspects of the earliest Triassic microbialites along the southern periphery of the tropical Yangtze Platform: initiation and cessation of a microbial regime. Palaios 23, 356–369.

Ezaki, Y., Liu, J.B., Adachi, N., 2012. Lower Triassic stromatolites in Luodian County, Guizhou Province, South China: evidence for the protracted devastation of the marine environments. Geobiology 10, 48–59.

Feldmann, R.M., Schweitzer, C.E., Hu, S.X., Zhang, Q.Y., Zhou, C.Y., Xie, T., Huang, J.Y., Wen, W., 2012. Macrurous Decapoda from the Luoping biota (Middle Triassic) of China. J. Paleontol. 86, 425–441.

Feldmann, R.M., Schweitzer, C.E., Hu, S.X., Huang, J.Y., Zhou, C.Y., Zhang, Q.Y., Wen, W., Xie, T., Maguire, E., 2015. Spatial distribution of Crustacea and associated organisms in the Luoping biota (Anisian, Middle Triassic), Yunnan Province, China: evidence of periodic mass kills. J. Paleontol. 89, 1022–1037.

Feng, X.Q., Chen, Z.Q., Woods, A., Fang, Y.H., 2017a. A Smithian (Early Triassic) ichnoassemblage from Lichuan, Hubei Province, South China: implications for biotic recovery after the latest Permian mass extinction. Palaeogeogr. Palaeoclimatol. Palaeoecol. 486, 123–141.

Feng, X.Q., Chen, Z.Q., Bottjer, D.J., Fraiser, M.L., Xu, Y.L., Luo, M., 2017b. Additional records of ichnogenus *Rhizocorallium* from the Lower and Middle Triassic, south China: implications for biotic recovery after the end-Permian mass extinction. GSA Bull. (in press).

Feng, X.Q., Chen, Z.Q., Woods, A., Wu, S.Q., Fang, Y.H., Luo, M., Xu, Y.L., 2017c. Anisian (Middle Triassic) marine ichnocoenoses from the eastern and western margins of the

Kamdian Continent, Yunnan Province, SW China: implications for the Triassic biotic recovery. Glob. Planet. Chang. 157, 194–213.

Feng, Z.Z., Bao, Z.D., Li, S.W., 1997. Lithofacies paleogeography of Middle and Lower Triassic of South China. Petroleum Industry Press, Beijing, pp. 1–222 (in Chinese with English abstract).

Fenton, C.L., Fenton, M.A., 1937. *Archaeonassa*, Cambrian snail trails and burrows. American Midland Naturalist 18, 454–456.

Fillmore, D.L., Lucas, S.G., Simpson, E.L., 2011. The fish swimming trace *Undichna* from the Mississippian Mauch Chunk Formation, Eastern Pennsylvania. Ichnos 18, 27–34.

Flügel, E., 2004. Microfacies of carbonate rocks: analysis, interpretation and application. Springer, New York, pp. 1–976.

Foster, W.J., Twitchett, R.J., 2014. Functional diversity of marine ecosystems after the Late Permian mass extinction event. Nat. Geosci. 7, 233–238

Fraiser, M.L., Bottjer, D.J., 2009. Opportunistic behavior of invertebrate marine tracemakers during the Early Triassic aftermath of the end-Permian mass extinction. Aust. J. Earth Sci. 56, 841–857.

Gibert, J.M.de., 2001. *Undichna gosiutensis*, isp. nov.: a new fish trace fossil from the Jurassic of Utah. Ichnos 8, 15–22.

Gibert, J.M.de., Martinell, J., 1996. Trace fossil assemblages and their palaeoenvironmental significance in the Pliocene marginal marine deposits of the Baix Ebre (Catalonia, NE Spain). Géologie Méditerranéenne 23, 211–225.

Gibert, J.M.de., 1996. A new decapod burrow system from the NW Mediterranean Pliocene. Revista Española de Paleontología 11, 251–254.

Gibert, J.M.de., Jeong, K., Martinell, J. 1999a. Ethologic and ontogenic significance of the Pliocene trace fossil *Sinusichnus sinuosus* from the northwestern Mediterranean. Lethaia 32, 31–40.

Gibert, J.M.de., Buatois, L.A., Fregenal-Martinez, M.A., Mangano, M.G., Ortega, F., Poyato-Ariza, F.J., Wenz, S., 1999b. The fish trace fossil *Undichna* from the Cretaceous of Spain. Palaeontology 42, 409–427.

Godbold, A., Schoepfer, S., Shen, S.Z., Henderson, C.M., 2017. Precarious ephemeral refugia during the earliest Triassic. Geology 45, 607–610.

Graham, J.R., Pollard, J.E., 1982. Occurrence of the trace fossil Beaconites antarcticus in the lower Carboniferous fluviatile rocks of county Mayo, Ireland. Palaeogeogr. Palaeoclimatol. Palaeoecol. 38, 257–268.

Grimm, K.A., Follmi, K.B., 1994. Doomed pioneers: allochthonous crustacean tracemakers in anaerobic basinal strata, Oligo-Miocene San Gregorio Formation, Baja California Sur, Mexico. Palaios 9, 313–334.

Hall, J., 1847. Paleontology of New York. Volumn 1, C. Van Benthuysen, Albany, 362 pp.

Häntzschel, W., 1975. Trace fossil and Problematica. In: Teichert, C. (ed.), Treatise on Invertebrate Paleontology, Part W, Miscellanea, Supplement I, Geological Society of America and University of Kansas Press, pp. 1–269.

Heer, O., 1877. Flora Fossilis Helvetiae. Vorweltliche Flora der Schweiz. J. Wurster & Comp., Zurich, 182 pp.

Hofmann, R., Goudemand, N., Wasmer, M., Bucher, H., Hautmann, M., 2011. New trace fossil evidence for an early recovery signal in the aftermath of the end–Permian mass extinction. Palaeogeogr. Palaeoclimatol. Palaeoecol. 310, 216–226.

Hofmann, R., Buatois, L.A., MacNaughton, R.B., Mangano, M.G., 2015. Loss of sedimentary mixed layer as a result of the end-Permian extinction. Palaeogeogr. Palaeoclimatol. Palaeoecol. 428, 1–11.

Hu, S.L., Li, Y.J., Dai, M., Pu, Z.P., 1996. The laser mass-spectrometer ^{40}Ar–^{49}Ar age of green pisolites of Guizhou Province. Acta Petrol. Sin. 12, 409–415 (in Chinese).

Hu, S.X., Zhang, Q.Y., Chen, Z.Q., Zhou, C.Y., Lv, T., Xie, T., Wen, W., Huang, J.Y., Benton, M.J., 2011. The Luoping biota: exceptional preservation, and new evidence on the Triassic recovery from end-Permian mass extinction. Proc. R. Soc. B 278, 2274–2283.

Huang, J.Y., Feldmann, R.M., Schweitzer, C.E., Hu, S.X., Zhou, C.Y., Benton, M.J., Zhang, Q.Y., Wen, W., Xie, T., 2013. A new shrimp (Decapoda, Dendrobranchiata, Penaeoidea) from the Middle Triassic of Yunnan, Southwest China. J. Paleont. 87, 603–611.

Huang, J.Y., Zhang, K.X., Zhang, Q.Y., Lv, T., Zhou, C.Y., Bai, J.K., 2009. Conodonts stratigraphy and sedimentary environment of the Middle Triassic at Daaozi Section of Luoping county, Yunnan province, South China. Acta Micropalaeontologica Sinica 26, 211–224 (In Chinese with English abstract).

Hull, P., Darroch, S.A.F., 2013. Mass extinction and the structure and function of ecosystem. In: Bush, A., Pruss, S.B., Payne, J.L. (Eds.), Ecosystem Paleobiology and Geobiology, The Paleontological Society Papers 19, 1–42.

Jame, N.P., Bourque, P.A., 1992. Reefs and Mounds. In: Walker, R.G., James, N.P (Eds.), Facies Models: response to sea level change. Geological Association of Canada, St. John's, pp. 323–348.

Keighley, D.G., Pickerill, R.K., 1994. The ichnogenus *Beaconites* and its distinction from *Ancorichnus* and *Taenidium*. Palaeontology 37, 305–337.

Knaust, D., 2007. Invertebrate trace fossils and ichnodiversity in shallow-marine carbonates of the German Middle Triassic (Muschelkalk). In: Bromley, R.G., Buatois, L.A., Mangano, G., Genise, J.F., Melchor, R.N., (Eds.), Sediment-Organism Interactions: a multifaceted ichnology. SEPM Special Publication 88, pp. 223–240.

Knaust, D., 2010. The end-Permian mass extinction and its aftermath on an equatorial carbonate platform: insights from ichnology. Terra Nova 22, 195–202.

Knaust, D., 2013. The ichnogenus *Rhizocorallium*: classification, trace makers, palaeoenvironments and evolution. Earth Sci. Rev. 126, 1–47.

Knaust, D., Uchman, A., Hagdorn, H., 2016. The probable isopod burrow *Sinusichnus seilacheri* isp. n. from the Middle Triassic of Germany: an example of behavioural convergence. Ichnos 24, 138–146.

Kotake, N., 1992. Deep-sea echiurans: possible producers of *Zoophycos*. Lethaia 25, 311–316.

Książkiewicz, M., 1968. O niektórych problematykach z fliszKarpat polskich, Częśc III. Rocznik Polskiego Towarzystwa Geologicznego 38, 3–17.

Książkiewicz, M., 1977. Trace fossils in the flysch of the Polish Carpathians. Palaeontol. Pol. 36, 1–208.

Lehrmann, D.J., Enos, P., Payne, J.L., Montgomery, P., Wei, J.Y., Yu, Y.Y., Xiao, J.F., Orchard, M.J., 2005. Permian and Triassic depositional history of the Yangtze platform and Great Bank of Guizhou in the Nanpanjiang Basin of Guizhou and Guangxi, South China. Albertiana 33, 149–168.

Lima, J.H., Netto, R.G., 2012. Trace fossils from the Permian Teresina Formation at Cerro Caveiras (S Brazil). Revista Brasileira de Paleontology 15, 5–22.

Liu, J., Hu, S.X., Rieppel, O., Jiang, D.Y., Benton, M.J., Kelley, N.P., Aitchison, J.C., Zhou, C.Y., Wen, W., Huang, J.Y., Xie, T., Lv, T., 2014. A gigantic nothosaur (Reptilia: Sauropterygia) from the Middle Triassic of SW China and its implication for the Triassic biotic recovery. Sci. Rep. 4, e7142.

Luo, M., 2014. Early Triassic trace fossils from South China: implications for biotic recovery from the end-Permian Mass Extinction. The University of Western Australia. Unpublished PhD thesis. 1–222.

Luo, M., Chen, Z.Q., 2014. New arthropod traces from the Lower Triassic Kockatea Shale Formation, northern Perth Basin, Western Australia: ichnology, taphonomy and palaeoecology. Geological J. 49, 163–176.

Luo, M., Chen, Z.Q., Hu, S.X., Zhang, Q.Y., Benton, M.J., Zhou, C.Y., Wen, W., Huang, J.Y., 2013. Carbonate reticulated ridge structures from the lower Middle Triassic of the Luoping area, Yunnan, southwestern China: Geobiologic features and implications for exceptional preservation of the Luoping Biota. Palaios 28, 541–551.

Luo, M., George, A.D., Chen, Z.Q., 2016. Sedimentology and ichnology of two Lower Triassic sections in South China: implications for the biotic recovery from the end-Permian Mass extinction. Glob. Planet. Chang. 144, 198–212.

Luo, M., Hu, S.X., Benton, M.J., Zhao, L.S., Huang, J.Y., Song, H.J., Wen, W., Zhang, Q.Y., Fang, Y.H., Huang, Y.G., Chen, Z.Q., 2017. Taphonomy and palaeobiology of early Middle Triassic coprolites from the Luoping biota, southwest China: implications for reconstruction of fossil food webs. Palaeogeogr. Palaeoclimatol. Palaeoecol. 474, 223–246.

MacEachern, J.A., Bann, K.L., Gingras, M.K., Zonneveld, J.P., Dashtgard, S.E., Pemberton, S.G., 2012. The ichnofacies paradigm. In: Knaust, D., Bromley, R.G., (Eds.), Trace Fossils as Indicators of Sedimentary Environments. Developments in Sedimentology 64, 103–138.

MacEachern, J.A., Bann, K.L., Pemberton, S.G., Gingras, M.K., 2007. The ichnofacies paradigm: high resolution paleoenvironmental interpretation of the rock record. In: MacEachern, J.A., Gingras, M.K., Pemberton, S.G. (Eds.), Applied Ichnology. SEPM Short Course Notes 52, 27–46.

Massalongo, A., 1855. *Zoophycos*, novum genus plantorum fossilium. Antonelli, Verona, 52 pp.

Mata, S.C., Bottjer, D.J., 2011. Origin of Lower Triassic microbialites in mixed carbonate–siliciclastic successions: ichnology, applied stratigraphy, and the end-Permian mass extinction. Palaeogeogr. Palaeoclimatol. Palaeoecol. 300, 158–178.

McBride, E.F., Folk, R.L., 1979. Features and origin of Italian Jurassic radiolarites deposited on continental crust. J. Sediment. Petrol. 49, 838–868.

McGhee, G.R., Sheehan, P.M., Bottjer, D.J., Droser, M.L., 2004. Ecological ranking of Phanerozoic biodiversity crises: ecological and taxonomic severities are decoupled. Palaeogeogr. Palaeoclimatol. Palaeoecol. 211, 289–297.

Melchor, R.N., Bromley, R.G., Bedatou, E., 2009. *Spongeliomorpha* in nonmarine settings: an ichnotaxonomic approach. Earth Environment. Sci. Trans. R. Soc. Edinburgh 100, 429–436.

Morrissley, L.B., Braddy, S.J., S.J., Bennett, J.P., Marriott, S.B., Tarrant, P.R., 2004. First trails from the Lower Old Red Sandstone of Tredomen Quarry, Powys, southeast Wales. Geological J. 38, 337–358.

Morrow, J.R., Hasiotis, S.T., 2007. Endobenthic response through mass extinction episodes: predictive models and observed patterns. In: Miller III, W. (Ed.), Trace Fossils: Concepts, Problems, Prospects. Elsevier, Amsterdam, pp. 575–598.

Myrow, P.M., 1995. *Thalassinoides* and the enigma of early Paleozoic open-framework burrow systems. Palaios 10, 58–74.

Nicholson, H.A., 1873. Contributions to the study of the errant annelids of the older Palaeozoic rock. Proc. R. Soc. London. 21, 288–290.

Olóriz, F., Rodríguez-Tovar, F.J., 2000. *Diplocraterion*: A useful marker for sequence stratigraphy and correlation in the Kimmeridgian, Jurassic (Prebetic Zone, Betic Cordillera, southern Spain). Palaios 15, 546–552.

Osgood, R.G., 1970. Trace fossils of the Cincinnati area. Palaeontographica Americana, 6, 277–444.

Pemberton,S.G., Frey, R.W., 1982. Trace fossil nomenclature and the *Planonites–Palaeophycus* dilemma. J. Paleontol. 56, 843–881.

Peters, S.E., 2008. Environmental determinants of extinction selectivity in the fossil record. Nature 454, 626–629.

Pietsch, C., Bottjer, D.J., 2014. The importance of oxygen for the disparate recovery patterns of the benthic macrofauna in the Early Triassic. Earth Sci. Rev. 137, 65–84.

Pruss, S.B., Bottjer, D.J., 2004. Early Triassic trace fossils of the Western United States and their implications for prolonged environmental stress from the end-Permian Mass Extinction. Palaios 19, 551–564.

Reineck, H.E., 1963. Sedimentgefüge im Bereich der südliche Nordsee. Abhandlungen Senckenbergischen Naturforsche de Gesellschaft, 505, 1–138.

Schweitzer, C.E., Feldmann, R.M., Hu, S.X., Huang, J.Y., Zhou, C.Y., Zhang, Q.Y., Wen, W., Xie, T., 2014. Penaeoid Decapoda (Dendrobranchiata) from the Luoping biota (Middle Triassic) of China: systematics and taphonomic framework. J. Paleontol. 88, 457–474.

Seilacher, A., 1974. Flysch trace fossils: evolution of behavioural diversity in the deep-sea. Neues Jahrbuch für Geologie und Paläontologie, Monatshefte 4, 233–245.

Sepkoski, J.J., Bambach, R.K., Raup, D.M., Valentine, J.W., 1981. Phanerozoic marine diversity and the fossil record. Nature, 293, 435–437.

Shi, G., Woods, A., Yu, M.Y., Wei, H.Y., 2015. Two episodes of evolution of trace fossils during the Early Triassic in the Guiyang area, Guizhou Province, South China. Palaeogeogr. Palaeoclimatol. Palaeoecol. 426, 275–284.

Sperling, E.A., 2013. Tackling the 99%: can we begin to understand the paleoecology of the small and soft-bodied animal majority? In: Bush, A., Pruss, S.B., Payne, J. (Eds.), Ecosystem Paleobiology and Geobiology. The Paleontological Society Papers 19, 77–86.

Stockar, R., 2010. Facies, depositional environment, and palaeoecology of the Middle Triassic Cassina beds (Meride Limestone, Monte San Giorgio, Switzerland). Swiss J. Geosci. 103, 101–119.

Taylor, A.M., Gawthorpe, R.L., 1993. Application of sequence stratigraphy and trace fossil analysis to reservoir description: Examples from the Jurassic of the North Sea. In Parker, J.R., ed., Petroleum Geology of Northwest Europe: Proceedings of the 4th Conference: Geological Society, London, 317–335.

Taylor, A.M., Goldring, R., 1993. Description and analysis of bioturbation and ichnofabric. J. Geol. Soc. 150, 141–148.

Torell, O.M., 1870. Petrificata Suecana Formationis Cambricae. Lunds Universitets Årsskrift, 6, 1–14.

Twitchett, R.J., 1999. Palaeoenvironments and faunal recovery after the end-Permian Mass Extinction. Palaeogeogr. Palaeoclimatol. Palaeoecol. 154, 27–37.

Twitchett, R.J., 2006. The palaeoclimatology, palaeoecology and palaeoenvironmental analysis of mass extinction events. Palaeogeogr. Palaeoclimatol. Palaeoecol. 232, 190–213.

Twitchett, R.J., Barras, C.G., 2004. Trace fossils in the aftermath of mass extinction events. In: McIlroy, D. (Ed.), Application of Ichnology to Palaeoenvironmental and Stratigraphic Analysis: Geological Society of London, Special Publication, 228, pp. 395–415.

Twitchett, R.J., Wignall, P.B., 1996. Trace fossils and the aftermath of the Permo–Triassic mass extinction: evidence from northern Italy. Palaeogeogr. Palaeoclimatol. Palaeoecol. 124, 137–151.

Uchman, A., 1995. Taxonomy and palaeoecology of flysch trace fossils: The Marnoso-arenacea Formation and associated facies (Miocene, Northern Apennines, Italy). Beringeria 15, 1–115.

Uchman, A., 1998. Taxonomy and ethology of flysch trace fossils: revision of the marian Książkiewicz collection and studies of complementary materials. Annales Societatis Geologorum Poloniae 68, 105–218.

Uchman, A., Hanken, N. M., Nielsen, J. K., Grundvåg, S.A., Piasecki, S., 2016. Depositional environment, ichnological features and oxygenation of Permian to earliest Triassic marine sediments in central Spitsbergen, Svalbard. Polar Res. 35, e24782.

Vossler, S.M., Pemberton, S.G., 1988. *Skolithos* in the Upper Cretaceous Cardium Formation: an ichnofossil example of opportunistic ecology. Lethaia 21, 351–362.

Walker, R.G., 1992. Turbidites and submarine fans. In: Walker, R.G., James, N.P (Eds.), Facies Models: response to sea level change. Geological Association of Canada, St. John's, pp. 239–264.

Wen, W., Zhang, Q.Y., Hu, S.X., Zhou, C.Y., Xie, T., Huang, J.Y., Chen, Z.Q., Benton,M.J., 2012. A new basal actinopterygian fish from the Anisian (Middle Triassic) of Luoping, Yunnan Province, Southwest China. Acta Palaeontol. Pol. 57, 149–160.

Wen,W., Zhang, Q.Y., Hu, S.X., Benton, M.J., Zhou, C.Y., Xie, T., Huang, J.Y., Chen, Z.Q., 2013. Coelacanths from the Middle Triassic Luoping biota, Yunnan, South China, with the earliest evidence of ovoviviparity. Acta Palaeontol. Pol. 58, 175–193.

Whidden, K.J., 1990. Preferential silicification of trace and body fossils in the Fossil Mountain Member of the Permian Kaibab Formation (southwestern Utah): Unpublished M.S Thesis, University of Southern California, Los Angeles, 158 pp.

Wignall, P.B., Hallam, A., Lai, X.L., Yang, F.Q., 1995. Palaeoenvironmental changes across the Permian/Triassic boundary at Shangshi (N. Sichuan, China). Historical Biol. 10, 175–189.

Wignall, P.B., Morante, R., Newton, R., 1998. The Permo–Triassc transition in Spitsbergen: δ^{13}Corg chemostratigraphy, Fe and S geochemistry, facies, fauna and trace fossils. Geol. Mag. 135, 47–62.

Wignall, P.B., Newton, R., 1998. Pyrite framboid diameter as a measure of oxygen deficiency in ancient mudrocks. Am. J. Sci. 298, 537–552.

Wilkin, R.T., Barnes, H.L., Brantley, S.L., 1996. The size distribution of framboidal pyrite in modern sediments: an indicator of redox conditions. Geochim. Cosmochim. Acta 60, 3897–3912.

Worsley, D., Mørk, A., 2001. The environmental significance of the trace fossil *Rhizocorallium jenense* in the Lower Triassic western Spitsbergen. Polar Res. 20, 37–48.

Yochelson, E.L., Fedonkin, M.A., 1997. The type specimens (Middle Cambrian) of the trace fossil *Archaeonassa* Fenton and Fenton. Can. J. Earth. Sci. 34, 1210–1219.

Zhang, Q.Y., Wen,W., Hu, S.X., Benton, M.J., Zhou, C.Y., Xie, T., Lu, T., Huang, J.Y., Choo, B., Chen, Z.Q., Liu, J., Zhang, Q.C., 2014. Nothosaur foraging tracks from the

Middle Triassic of Southwestern China. Nat. Commun. 5, 3973e, DOI: 10.1038/ncomms4973.

Zhang, Q.Y., Zhou, C.Y., Lu, T., Xie, T., Lou, X.Y., Liu, W., Sun, Y.Y., Wang, X.S., 2008a. Discovery and significance of the Middle Triassic Anisian Biota. Geol. Rev. 54, 523–527 (in Chinese with English abstract).

Zhang, Q.Y., Zhou, C.Y., Lu, T., Xie, T., Lou, X.Y., Liu, W., Sun, Y.Y., Huang, J.Y., Zhao, L.S., 2009. A conodont-based Middle Triassic age assignment for the Luoping Biota of Yunnan, China. Science in China Series D: Earth Sciences 52, 1673−1678.

Zhang, L.J., Fan, R.Y., Gong, Y.M., 2015. *Zoophycos* macroevolution since 541 Ma. Sci. Rep. 4, e14954.

Zhang, X.H., Shi, G.R., Gong, Y.M., 2008b. Middle Jurassic trace fossils from the Ridang Formation in Sajia County, South Tibet, and their palaeoenvironmental significance. Facies 54, 45–60.

Zhao, X.M., Tong, J.N., 2010. Two episodic changes of trace fossils through the Permian-Triassic transition in the Meishan cores, Zhejiang Province. Sci. China Ser. D Earth Sci. 53, 1885–1893.

Zhao, X.M., Tong, J.N., Yao, H.Z., Niu, Z.J., Luo, M., Huang, Y.F., Song, H.J., 2015. Early Triassic trace fossils from the Three Gorges area of South China: implications for the recovery of benthic ecosystems following the Permian-Triassic extinction. Palaeogeogr. Palaeoclimatol. Palaeoecol. 429, 100–116.

Zenker, J.C., 1836. Historisch-topographisches Taschenbuch von Jena und seiner Umgebung. Friedrich Frommann, Jena. 1–338.

Zonneveld, J.P., 2011. Suspending the rules: unravelling the ichnological significance of the Lower Triassic post-extinction recovery interval. Palaios 26, 677–681.

Zonneveld, J.P., Gingras, M.K., Pemberton, S.G., 2001. Trace fossil assemblages in a Middle Triassic mixed siliciclastic–carbonate marginal marine coastal depositional system, British Columbia. Palaeogeogr. Palaeoclimatol. Palaeoecol. 166, 249–276.

Zonneveld, J.P., Gingras, M.K., Beatty, T.W., 2010. Diverse ichnofossil assemblage following the P-T mass extinction, Lower Triassic, Alberta and British Columbia, Canada: evidence for shallow marine refugia on the northwestern coast of Pangaea. Palaios 25, 368–392.

Figure and Figure captions

Fig. 1.A, Location of the three studied sections (stars) at Luoping, Yunnan Province of South China. Note the insert map (B) only shows mainland China. B, Middle Triassic palaeogeographic map of South China showing the palaeogeographic setting of Luoping and adjacent areas [base map modified from Feng et al., (1997)].

Fig. 2. Stratigraphic columns showing the distribution of trace fossils and bioturbation levels of the three studied representative sections at Luoping, Yunnan Province. The bioturbation scheme follows Reineck (1963) and Taylor and Goldring (1993). Abundant invertebrate and vertebrate fossils occur in the Dawazi, Xiangdongpo, and Shangshikan sections, which are abbreviated as DWZ, XDP, and SSK, respectively. Note, the nodular, bioturbated carbonate wackestone is here applied as a marker bed to correlate the trace fossil records of the three sections.

Fig. 3. Field photos showing the typical rock types and sedimentary structures within each unit of the three sections. A, oncoidal packstone-wackestone, bed 2, XDP. Note the individual oval to irregular shaped oncoids (arrowed); B, laminated marly carbonate mudstone, bed 26–27, SSK. Note the very thin-bedded chert layers (arrowed) intercalated in marly carbonate mudstone. Hammer is 39 cm long; C, plan view of carbonate reticulated ridge structures. Bed 88, XDP; D, Turbidite deposits from the XDP section, bed 55. The sharp-based, normally graded wacke-packestone layer is overlain by very thin layers of planar- to convolute-laminated carbonate mudstone and structureless carbonate mudstone. They are here interpreted to represent Ta, Tb+Tc and Te of the Bouma turbiditic sequence. E, nodular carbonate wackestone and overlying marly carbonate mudstone. XDP, bed 73 and 74. F, Hummocky cross-stratified carbonate wackestone; XDP, bed 136. G, thick-bedded carbonate mudstone, with planar lamination. XDP, bed 167 and 168. H, laminated stromatolitic dolomite, bed 187, DWZ.

Fig.4. Field photos showing trace fossils from the Middle Triassic Guanling Formation. A, Horizontal *Archaeonassa* (arrowed); bed 9, SSK; B, *Arenicolites*; bed 2, XDP; C, *Dikoposichnus*; bed 34, SSK; Note the two black arrows indicating the single imprints made by animal limbs. White arrow indicates direction of movement of the trace maker. D–E, Enlargement of *Diplocraterion* isp. from bed 42, SSK. Note the paired tube with spreiten,

characterizing *Diplocraterion*. F, Dense *Diplocraterion* isp. preserved on thin-bedded carbonate mudstone, bed 42, SSK; G, *Megagrapton irregulare*, bed 42, DWZ.

Fig. 5. Field photos showing trace fossils from the Middle Triassic Guanling Formation. A, *Palaeophycus,* bed 172, XDP; B, *Planolites*, bed 171, SSK; C, *Rhizocorallium* isp.; bed 168, XDP; D, *Rhizocorallium commune*, bed 71, XDP. E, *Rhizocorallium commune,* bed 70, DWZ. F, detail showing the faecal pellets in marginal tubes of *R. commune.* G, *Sinusichnus* isp.*,* bed 40, XDP. Note the Y-shaped (white arrow) and T-shaped (black arrow) branchings in burrow system. H is a sketch of G showing the overall morphology of *S.* isp..

Fig. 6. Field photos showing trace fossils from the Middle Triassic Guanling Formation. A, *Spongeliomorpha* isp., bed 9 SSK. Note the longitudinal scratch marks on burrow surface (white arrows). B, *Taenidium barretti*, bed 35, SSK; C, *Thalassinoides suevicus*, bed 34, SSK. Note the swelling and Y-shaped branching in *Thalassinoides suevicus* (arrows). D, *Undichna unisulca*, Bed 105, DWZ; E, *Zoophycos* isp. ?; Guangling Formation, Boyun; F, *Zoophycos* isp., DWZ; Coin is 2.5 cm in diameter, DWZ.

Fig. 7. Burrow size measurements of commonly occurring trace fossils at Luoping, Yunnan Province. A, *Planolites*, bed 171, XDP; B, large sized *Rhizocorallium commune*, isp., bed 36, XDP; C, small sized *Rhizocorallium* isp., bed 168, XDP; D, *Thalassinoides suevicus*, Bed 34, SSK.

Fig. 8. Statistical analysis of pyrite framboids from fossil beds of the Luoping Biota. A, SEM photo showing pyrite framboids from marly carbonate mudstone, bed 15, SSK section. Note the abundant pyrite framboids (black arrows) of similar sizes occurring densely. B, Histogram showing the distribution of diameters of pyrite framboids for rock samples from the same bed. C, SEM photo of framboid pyrite from carbonate mudstone, bed 33, SSK. D, Histogram showing the diameter distribution of pyrite framboids for rock samples of the same bed MD = mean diameter; SD = standard deviation.

Fig. 9. Burrow size comparison of typical ichnotaxa from latest Permian to Middle Triassic. A, *Planolites*; B, *Rhizocorallium*; C. *Thalassinoides*; Changh.: Changhsingian; Grie.: Griesbachian; Die.: Dienerian.

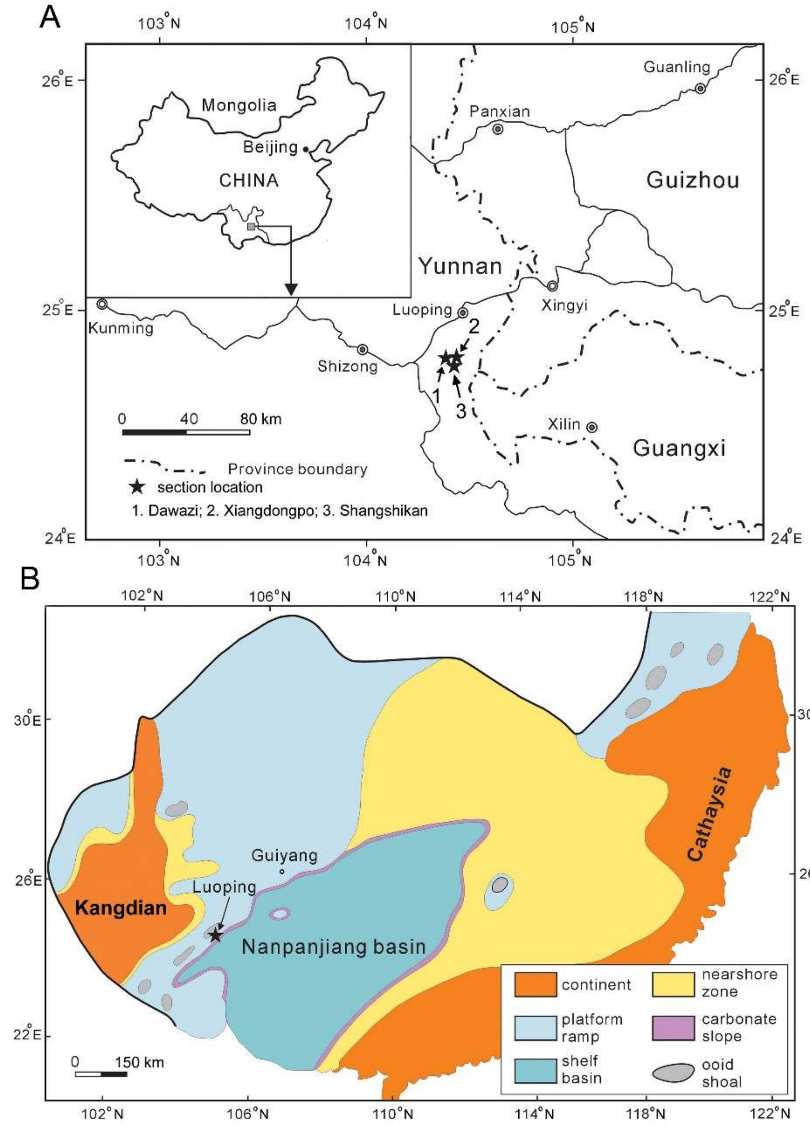
A
103°N
104°N
105°N
26°E
25°E
24°E
Mongolia
Beijing
CHINA
Guanling
Panxian
Guizhou
Yunnan
Xingyi
Luoping
Kunming
Shizong
Xilin
Guangxi
1
2
3
0
40
80 km
Province boundary
section location
1. Dawazi; 2. Xiangdongpo; 3. Shangshikan
B
102°N
106°N
110°N
114°N
118°N
122°N
30°E
26°E
22°E
Kangdian
Cathaysia
Guiyang
Luoping
Nanpanjiang basin
0
150 km
continent
nearshore zone
platform ramp
carbonate slope
shelf basin
ooid shoal

Figure 1

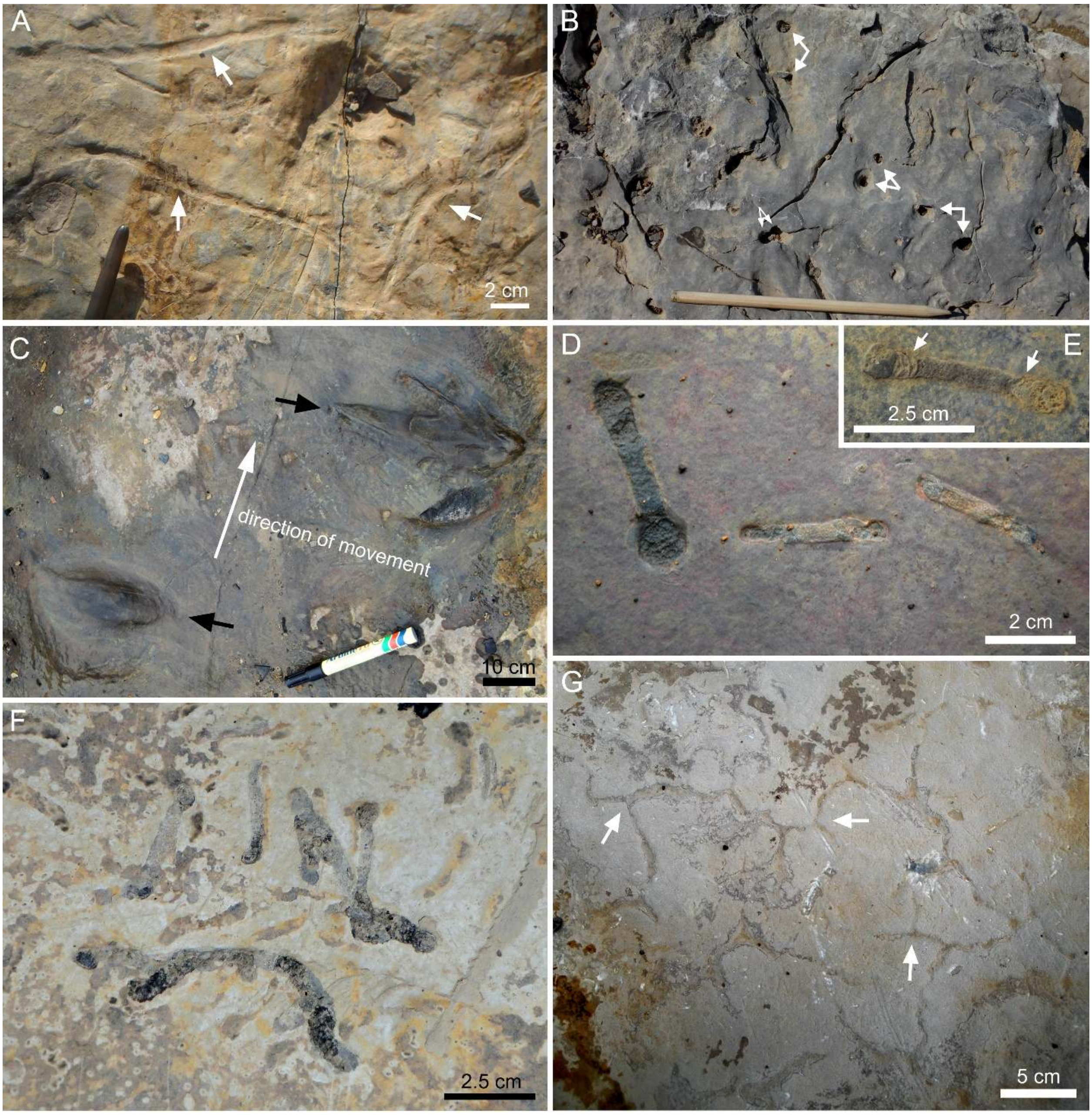

Figure 4

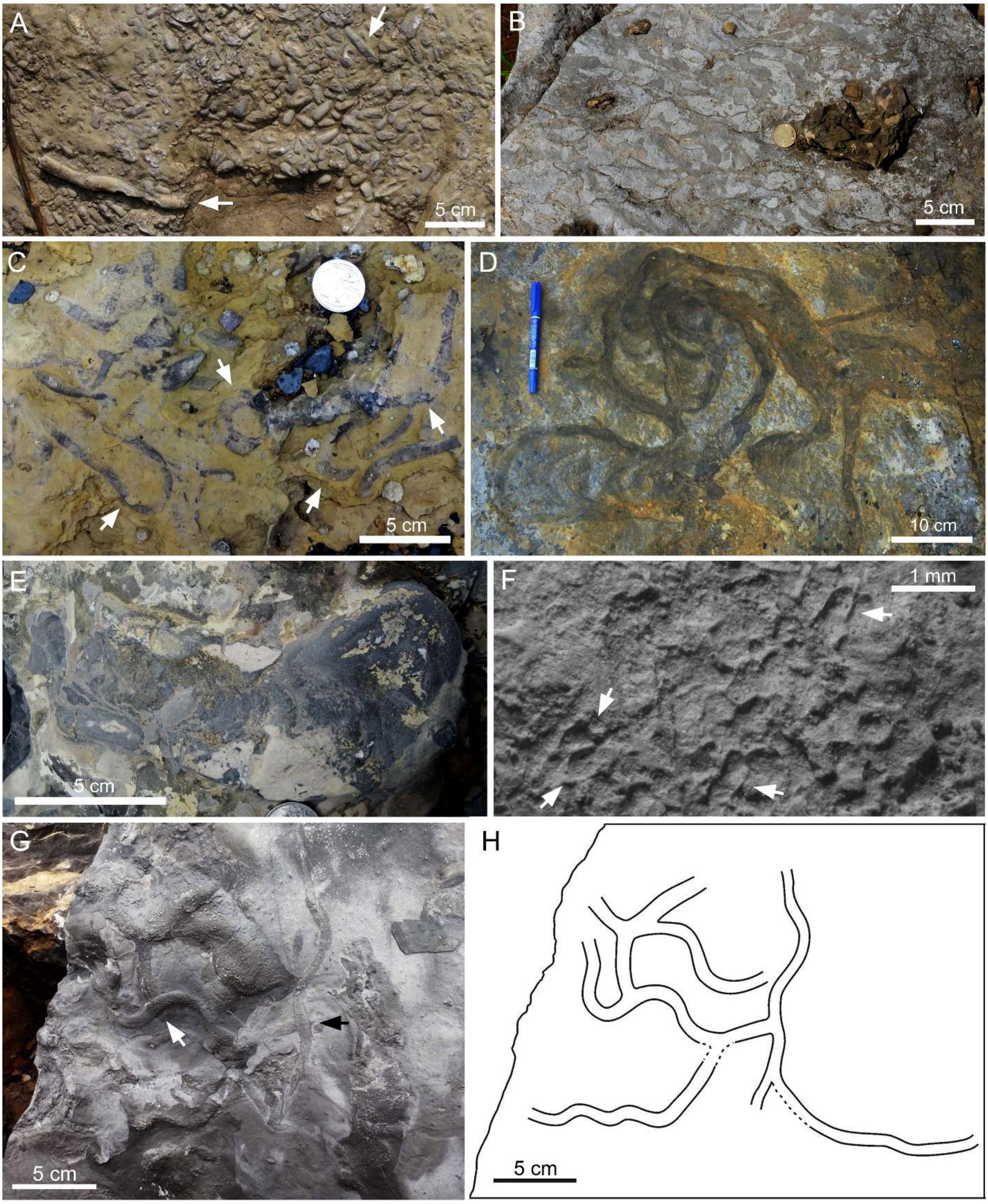

Figure 5

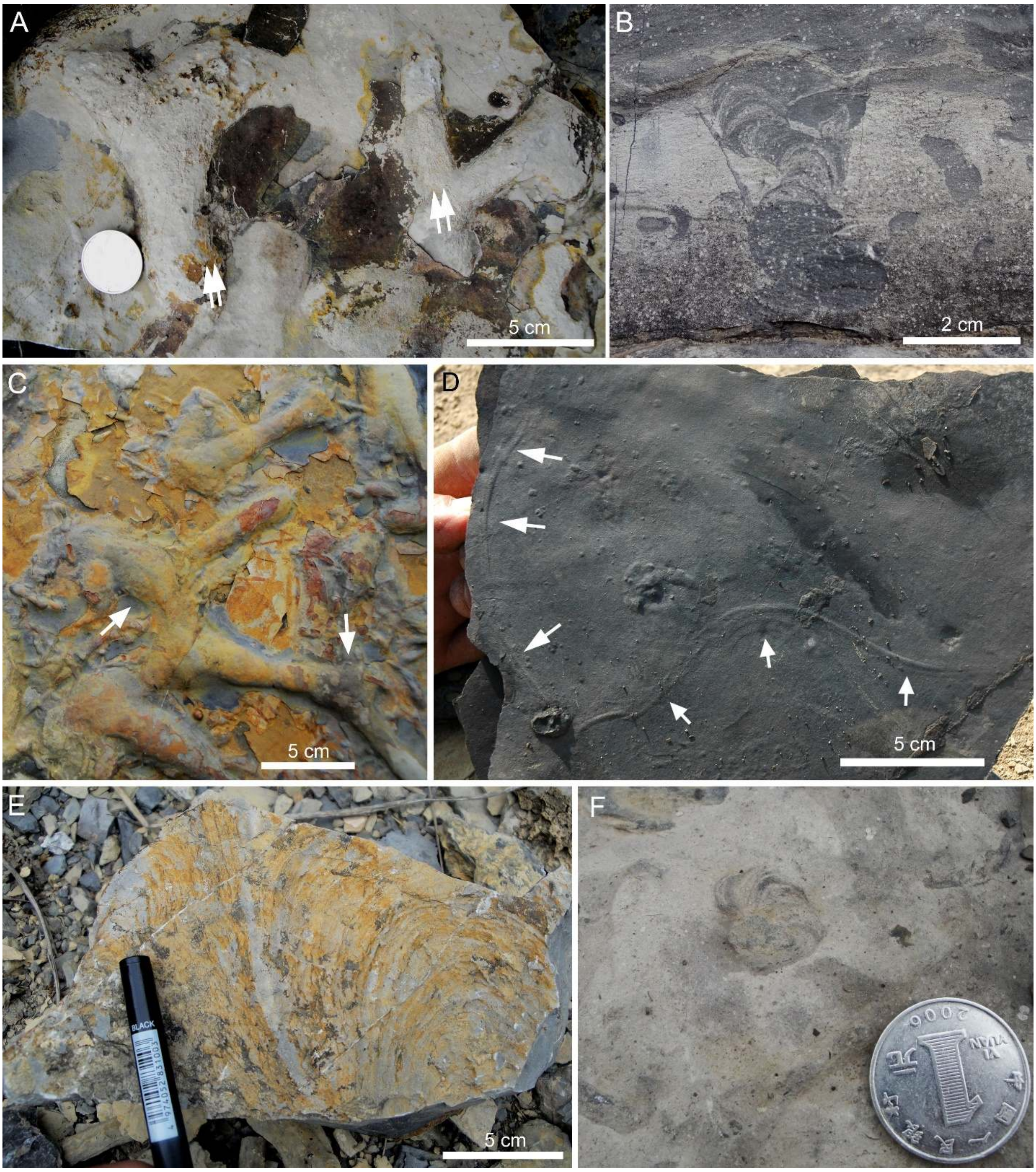

Figure 6